Process Chain Forming to Crash:

Efficient Stochastic Analysis

Tanja Clees[1], Daniela Steffes-lai[1], Martin Helbig[2], Karl Roll[3], Markus Feucht[3]

[1]Fraunhofer Institute for Algorithms and Scientific Computing SCAI, Sankt Augustin, Germany

[2]Fraunhofer Institute for Mechanics of Materials IWM, Freiburg, Germany

[3]Daimler AG, Sindelfingen, Germany

Summary:

During the fabrication of products, important material and process parameters, geometry and also external influences (e.g. room temperature) can vary considerably. It is known that they can have a substantial, even critical influence on the quality of the resulting products. Therefore, software tools and strategies supporting an efficient and thorough analysis of sensitivity, stability and robustness aspects as well as a multi-objective robust design-parameter optimization are necessary. This is especially true for parts of a car with a potentially critical influence in crashes as, for instance, the B-pillar which consists of several formed and connected blanks.

We propose a new strategy, built upon several software tools as well as new material models, supporting an analysis of variations for the process chain forming to crash. The strategy roughly consists of the following parts and software tools:

- forming simulation (LS-DYNA)
  - parameter sensitivity analysis (DesParO)
  - reduction/compression of input and output (DesParO)
- mapping (SCAImapper)
- crash simulation (LS-DYNA)
  - stability analysis (DIFF-CRASH)
  - sensitivity analysis (DesParO)
  - reduction/compression of input and output (DesParO)
- multi-objective robust design-parameter optimization (DesParO)
- comparisons with physical experiments (as far as available)

Efficient, novel methods are proposed and employed for sensitivity analysis of simulation results on fine grids depending on parameter variations, for a reduction of the design space and the simulation results as well as for mapping an appropriately constructed data base of most influencing trends, not only comprised of thicknesses and strains, but also damage information. Including the latter turns out to be a crucial point. Results are shown, in particular, for a ZStE340 metal blank of a B-pillar. Comparisons to experiments demonstrate the abilities of the strategy proposed.

Keywords:

forming simulation, crash simulation, process chain forming to crash, statistical analysis for random fields, robust design, sensitivity analysis, multi-objective robust design-parameter optimization.

1 Process Chain Forming to Crash: Outline

In this paper, software tools and strategies supporting an efficient and thorough analysis of sensitivity, stability and robustness aspects as well as a multi-objective robust design-parameter optimization are discussed. We propose a new strategy, built upon several software tools (see list below and Figure 2) as well as new material models (cf. Section 4.1), supporting an analysis of variations for the process chain forming to crash. The strategy comprises the following steps:

- **forming simulation** (see Section 2)
  - setup of appropriate input
  - parameter sensitivity analysis
  - "physical" reduction/compression of design parameters and data bases of simulation results
- **mapping** (see Section 3)
  - techniques for mapping one source file to one target file
  - techniques for mapping data bases
- **crash simulation** (see Section 4)
  - stability analysis
  - sensitivity analysis
  - reduction of number of necessary simulation runs
  - "physical" compression of data bases of simulation results
  - robustness analysis
- **multi-objective robust design-parameter optimization** (cf. Section 5)
- **comparisons with physical experiments** (see Sections 2 and 4)

The following software tools are used:
- LS-DYNA
- DesParO (new features, see [1], [4], and references given therein)
- DIFF-CRASH (see [6], [4], and references given therein)
- SCAImapper (see [4], and references given therein)

Optionally, FEMZIP [7] technologies can be used.

Efficient, novel methods are proposed and employed, particularly for
- analyzing sensitivities of simulation results on fine grids (here: thicknesses, strains, damages resulting from the forming process as well as output from the crash simulation) on parameter variations (here: relevant parameters of the forming process), and robustness aspects. The strategy proposed considerably differs from e.g. [8], especially due to the fact that large "random fields" are directly analyzed. Both local and global impacts can be analyzed here.
- reducing the design space and physically compressing simulation results (per process step)
- mapping an appropriately constructed data base of most influencing trends, here comprised of thicknesses, strains, and damage information. Including the latter turns out to be a crucial point.
- characterization of material behavior and physical tension-bending experiments.

Results are shown, in particular, for a ZStE340 metal blank of a B-pillar. Comparisons to experiments demonstrate the abilities of the strategy proposed. The paper concludes with an outlook on further analysis steps.

Figure 1: Part of the B-pillar considered for experiments and simulations: ZStE340 metal blank.

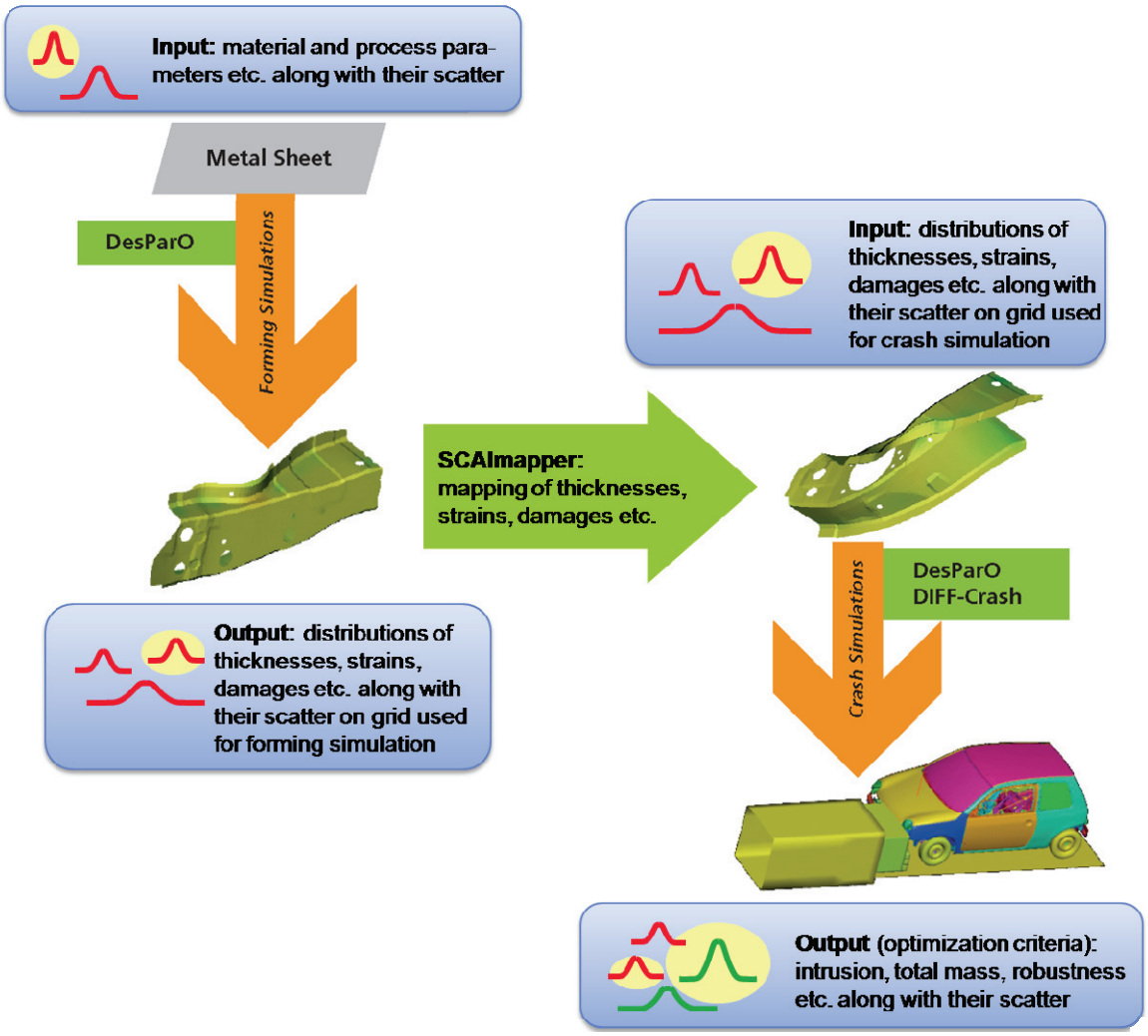

Figure 2: Process chain forming to crash: simulation types (in orange), typical kinds of variations to be dealt with (in blue), software tools (in green) supporting sensitivity and robustness analysis as well as multi-objective robust optimization (DesParO), mapping (SCAImapper) and a backtracking of instabilities in crash simulations (DIFF-CRASH). For forming and crash simulations, LS-DYNA is employed.

2 Forming: Simulation and Analysis

In the following, a brief outline of the model and tools employed for forming simulation as well as a discussion of analysis results is given.

2.1 Simulation Setup

The forming simulations are carried out by means of LS-DYNA. The simulation setup of the forming step as well as the resulting geometry and thickness of the basic model (without parameter variations) after forming are shown in Figure 3.

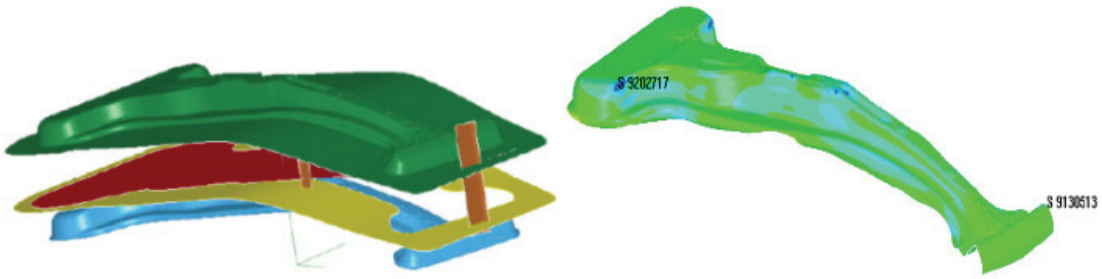

Figure 3: Blank before the forming process (left) and after forming (right).

2.2 Parameter Sensitivity Analysis and Reduction of the Design Space

2.2.1 Input and Output

A sensitivity analysis is carried out for a user-defined set of parameters together with a range of admissible values each, representing reasonable variations in practice (cf. Section 4.1, for instance). The following 9 parameters have been analyzed for the ZStE340 blank in a first step:

- 6 material parameters: E0, P1, P2 (swift law), R00, R45, R90 (anisotropy coefficients)
- 3 process parameters: MUE (friction), FORCFN (binder), DFSCL (drawbead).

Here, the sensitivity analysis is based on the following three output functionals (simulation results given on the grids resulting from the forming simulations):

- thicknesses
- effective plastic strains
- damages

The sensitivity analysis will be extended to cover a larger number of parameters (along with statistical information) as soon as the simulation models have been refined (see Section 4.1, for instance).

2.2.2 Steps and results of the analysis process

By using DesParO's novel sensitivity analysis tool (cf. [4]) for the case of relating *sets of scalar parameter values* to *data (simulation results) on fine grids*, the following steps are carried out:

1. A first design of experiments (**DoE)** is proposed consisting of ***2n+1*** simulation runs (minimum: n+1) for ***n*** being the number of parameters.
2. The corresponding (LS-DYNA) **simulation runs** are performed by means of a(ny standard) workflow software tool to feed the data base.
3. Efficient novel **parameter sensitivity analysis** for the whole data base by means constructing most important trends. The run time is just determined by reading and writing data. Core computational time is below a second on a standard computer. The data are not collectively read into memory, but processed "on the fly" instead. This way, huge data bases can be processed quickly on standard computing equipment.
4. **Classification of nonlinearity**: If the influences are too nonlinear, some more simulations are requested (iteratively extended DoE; go to step 2). This way, the number of simulation runs is minimized.
5. **Importance classification and reduction of the design space** (for continued analysis of the process chain and/or optimization): 3 parameters are the most influencing ones here ("first-level" importance), 2 are of a considerably lower, "second-level" importance, 4 are just of low, "third-level" importance.
6. **Reduction ("physical" compression) of the simulation data base**. The user can control the accuracy by defining residual measures. Here, the data base can be compressed to a file of basically the size of 2-3 times one simulation result (depending on accuracy requirements).
7. A further **compression** can be achieved by employing FEMZIP.
8. For the process chain: **Preparation of the data base** for the mapping process by means of a novel mechanism for constructing "relevant" simulation data (here: thicknesses, strains, damages).

3 Mapping Process

The mapping itself is carried out with the SCAImapper. Necessary steps for mapping a data base are indicated and the different mapping scenarios employed for preparing crash input are described.

3.1 SCAImapper

3.1.1 Defining Source and Target Geometries

Two basic geometries (along with their grids) are needed for the mapping processes, carried out by means of the SCAImapper. The source grid is obtained as output of the basic forming simulation, the target grid is the one specified for the basic crash simulation model. As usually, the crash grid is coarser than the grid resulting from the forming simulation. In addition, several parts have been cut out. The grid resulting from the LS-DYNA forming simulation runs is locally refined compared with the input grid, and grids resulting from LS-DYNA runs with different parameter sets (see Section 2.2) are even differently refined.

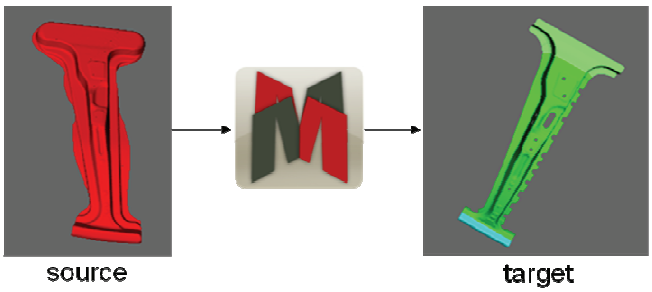

Figure 4: Source (left) and target (right) geometry for the mapping processes.

3.1.2 Mapping of One Source

The four steps for mapping data on one source to one target grid are depicted in Figure 5. The (manually controllable) rough alignment is important for a general orientation (especially rotations, mirroring) of the two models to each other, whereas the fine alignment is performed automatically.

3.1.3 Mapping of a Data Base

When mapping data bases, the same fine orientation of the source and target geometries have to be used in order to avoid the introduction of additional variations. In this context, the SCAImapper has been extended with a corresponding feature. A local evaluation of the mapping accuracy will be introduced, particularly to determine additional variations coming from the mapping process.

3.2 Mapping Scenarios Employed

Several mapping scenarios are employed in order to obtain suitable input for the crash simulation as well as to analyze effects of taking into account local thicknesses, strains, and/or damages. The following scenarios are discussed below:

1. Using homogeneous thicknesses, strains, and damages: Section 3.2.1.
2. Mapping local thicknesses, and using homogeneous strains and damages: Section 3.2.2.
3. Mapping local thicknesses and strains, and using homogeneous damages: Section 3.2.3.
4. Mapping local thicknesses, strains and damages: Section 3.2.4.

Results discussed in Section 4 show that all information as given by the last option should be taken into account in order to improve quality of the crash simulations as well as the overall process considerably.

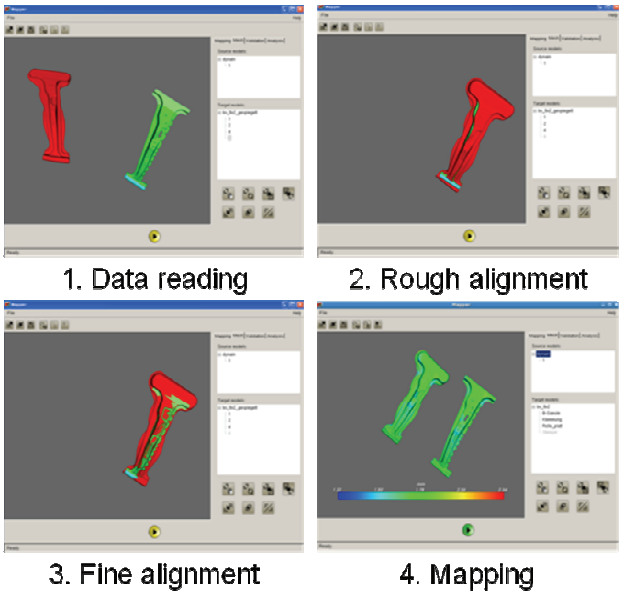

Figure 5: The four general steps for mapping data one one source to one target geometry.

3.2.1 Mapping Scenario "Global Values"

In Figure 6 and Figure 7, the first mapping scenario, "global values", is depicted.

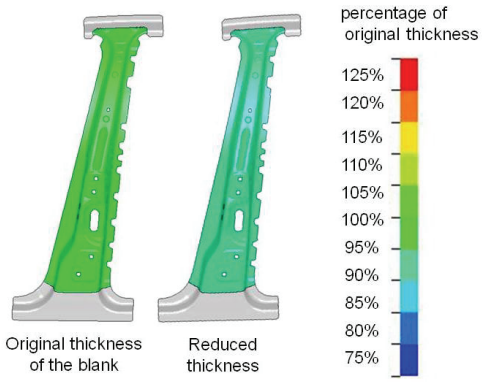

Figure 6: For the simulation with homogeneous parameters the thickness of the blank was reduced to 93% of the initial thickness of the sheet.

3.2.2 Mapping Scenario "Local Thicknesses"

The second mapping scenario, "local thicknesses", uses homogeneous strains and damages as depicted in Figure 7 and mapped thicknesses as depicted in Figure 8 (left).

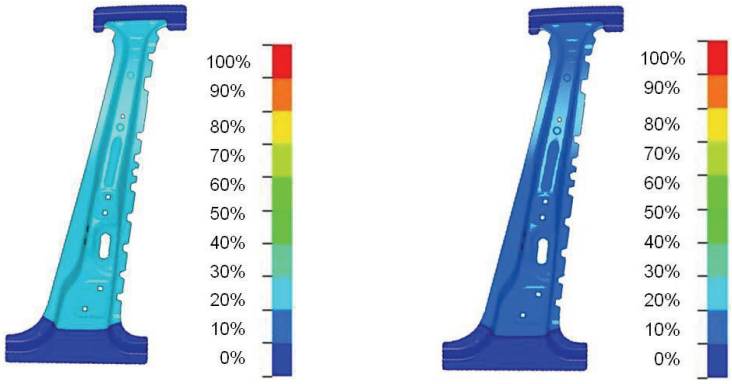

Figure 7: For simulations with homogeneous parameters: the initial plastic strain of the blank was set to 23% of the maximal strain from forming simulation (left), the initial damage was set to 13% (right), elements fail at 100%.

3.2.3 Mapping Scenario "Local Thicknesses and Strains"

The third mapping scenario, "local thicknesses and strains", uses homogeneous damages as depicted in Figure 7 (right) and mapped thicknesses and strains as depicted in Figure 8.

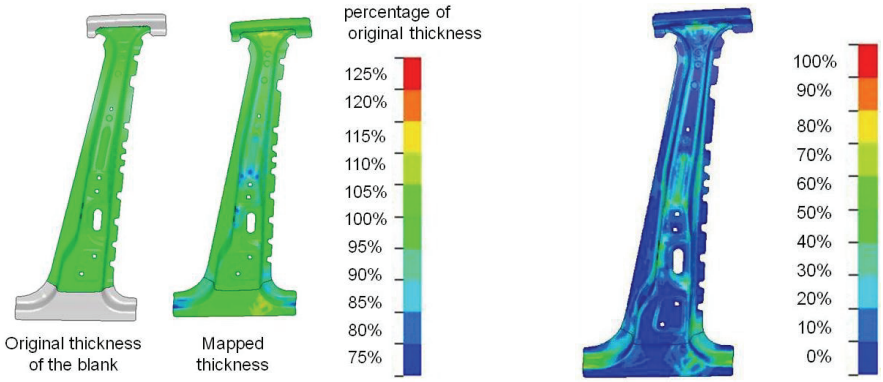

Figure 8: On the left: Change of thickness is mapped on the crash model. Percentage is for thickness of the original blank before the forming simulation. On the right: Plastic strain mapped on the blank: 0% means no plastic strain from forming simulation and 100% maximum plastic strain from forming simulation etc.

3.2.4 Mapping Scenario "Local Thicknesses, Strains and Damages"

For the fourth mapping scenario, "local thicknesses, strains and damages", mapped thicknesses and strains as depicted in Figure 8 are used (local damages are not shown here).

4 Characterization of Material Behavior, Crash Simulation and Analysis

In this chapter the characterization of the material behavior, the experimental test setup for the ZStE340 blank, the corresponding FE-model, and the analysis steps for the crash simulations are discussed.

4.1 Characterization of material behavior

4.1.1 Stochastic and deterministic diffusion

Two kinds of diffusion are considered. The stochastic diffusion is determined by smooth tension specimen tests. In Figure 9 (left) the distribution of the fracture strain at one of the three positions on

the formed metal blank is shown. The three positions and the deterministic influence of the forming process are shown in Figure 9 (right).

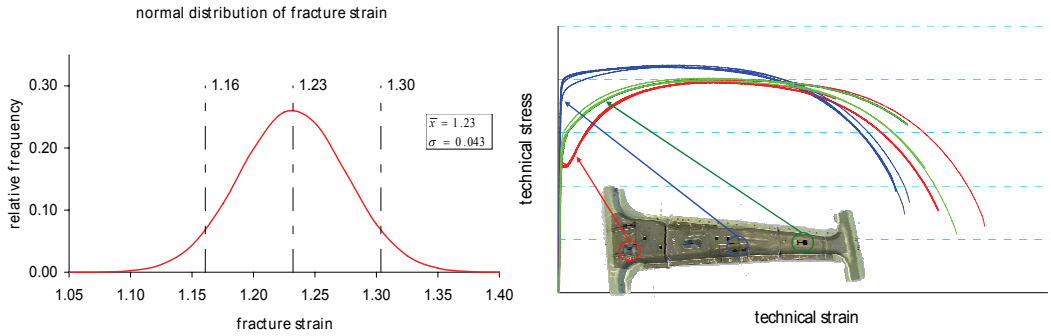

Figure 9: Stochastic diffusion of the fracture strain (left) and deterministic diffusion from forming process (right).

Figure 10 shows the technical stress-strain curves of tensile specimens from different positions and simulation results under consideration of initial strain, reduced shell thickness and initial failure. A good agreement between experiments and simulation can be seen. The consideration of deterministic influence of the forming process in crash simulation yields a more realistic result of the crash simulation.

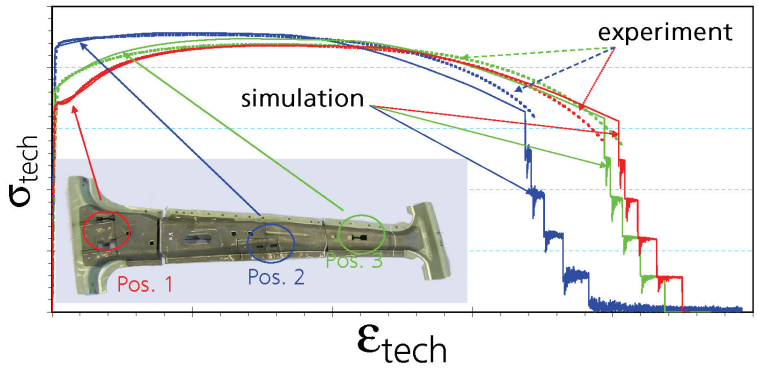

Figure 10: Results of experiments (dotted lines) along with simulation results (solid lines) for three positions on the blank.

4.1.2 Determination of the stress-strain curves

To minimize the influence of the deterministic diffusion the unformed sheet was used to characterize the material. For the determination of the yield curve the true stress-strain curves of smooth tension specimens, taken in the rolling direction, were used. Tension tests with different angles (0°,45°,90°) to the rolling direction were used to determine the anisotropy coefficients [11]. The influence of specimen orientation is shown in Figure 11.

4.1.3 Determination of the damage evolution

For the determination of the failure curve six different specimens with different stress triaxialities were used, as shown in Figure 12. The failure curve in Figure 12 does not consider the lower fracture strain under shear stress [10].

The simulation of the forming process and the crash simulation were done by using an isotropic material model with the Johnson-Cook failure criterion [9]. The Johnson-Cook failure strain was scaled versus the element length.

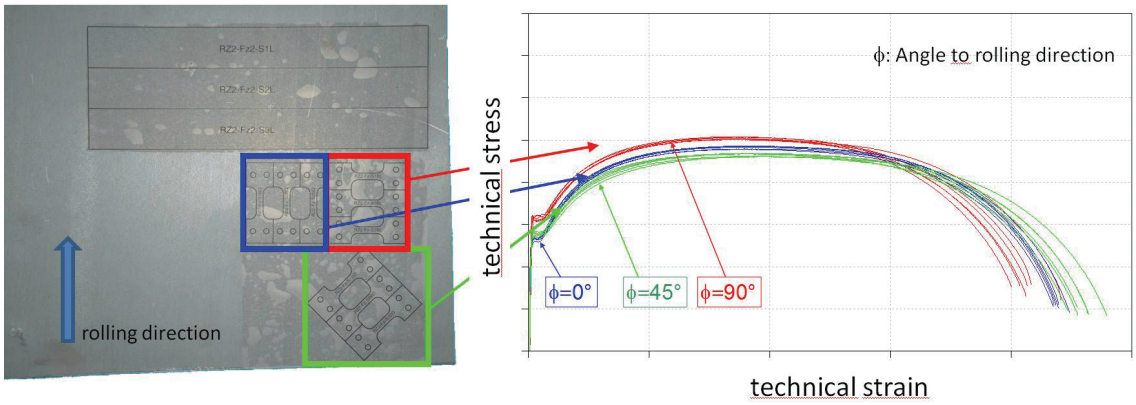

Figure 11: Specimen extraction from unformed sheet of ZStE340 (left). Technical stress-strain curves of tension specimens in different angles to the rolling direction (right).

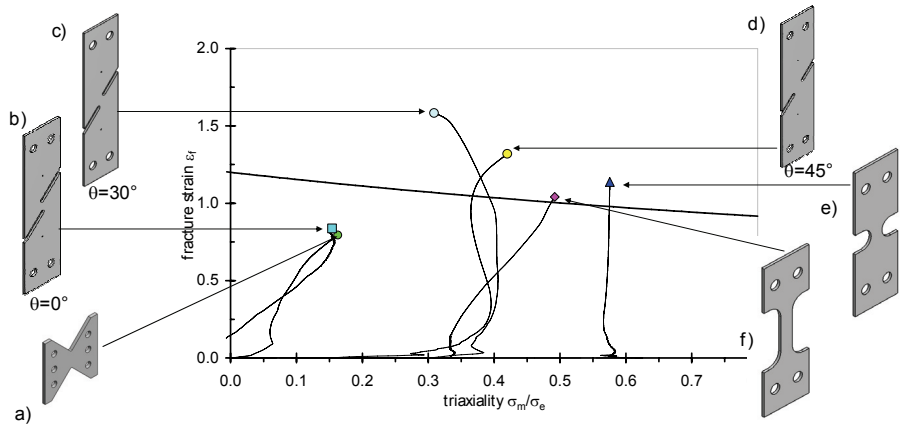

Figure 12: Fracture strain ε_f as function of stress triaxiality σ_m/σ_e using the Johnson-Cook Failure criterion: a) Arcan shear, b) shear tension θ=0°, c) shear tension θ=30°, d) shear tension θ=45°, e) notched tension, f) smooth tension.

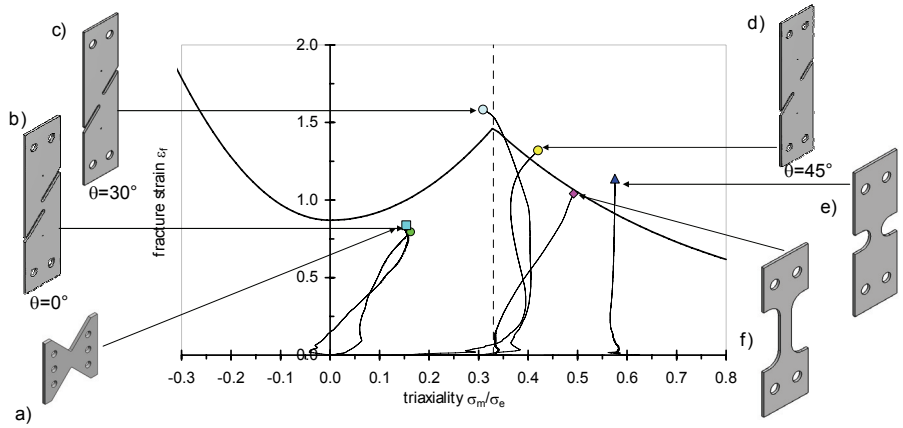

Figure 13: Fracture strain ε_f as function of stress triaxiality σ_m/σ_e with an extended Failure criterion.

In further investigations of the material and process parameters the failure criteria should consider the lower failure strains at lower triaxialities. An extended failure curve is shown on Figure 13. For considering the anisotropic material behavior of ZStE340 the material model will be changed to an

anisotropic material model with a damage evaluation (DAIMLER GISSMO [12]), which is able to calculate with the determined failure curve.

4.2 Experimental set-up of the ZStE340 metal blank test

To achieve a combination of bending with superposed tension in the component test, the blank was supported at both ends by revolvable bearings. The load application occurred path controlled, see Figure 14. The force and the path of the indenter are measured; additionally the test was recorded for visual analysis of the deformation and failure.

4.3 FE- Model of the tension-bending test

The FE-model, see Figure 15, consists of Belytschko-Tsay shell elements. The supports are modeled with rigid shell elements, which are turnable around the axes of the rolls, cf. Figure 14. A comparison of the experiments and simulation is shown in Figure 16 and Figure 17 (see below).

Figure 14: Experimental set-up of the tension-bending test on ZStE340 metal blank of a b-pillar.

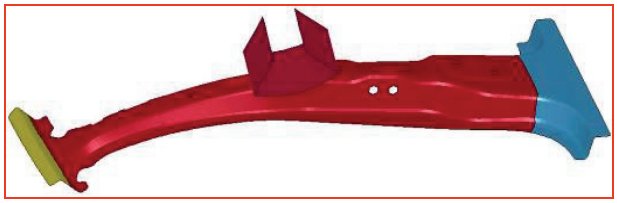

Figure 15: FE-Model of the tension-bearing test

4.4 First Comparisons with physical experiments

4.4.1 Taking the Mapping Scenario "Global Values" into Account

Figure 16 shows the force-displacement curve of a simulation with the assumption of a homogeneous distribution of parameters to consider the influence of the forming process. It can be seen, that the calculated forces are too high, and the difference in force between experiment and simulation is increasing at higher displacements, therefore a mapping process is necessary to consider local influences.

4.4.2 Taking the Mapping Scenario "Local Thicknesses, Strains (and Damages)" into Account

According to Figure 17, it can be seen, that the forming process has an influence on the results of the crash simulation. The influence of the mapped plastic strain can be seen in the higher force level. Compared to Figure 16, it shows also a better agreement at higher displacements, which is caused by (a first) consideration of the pre-damage from the forming process.

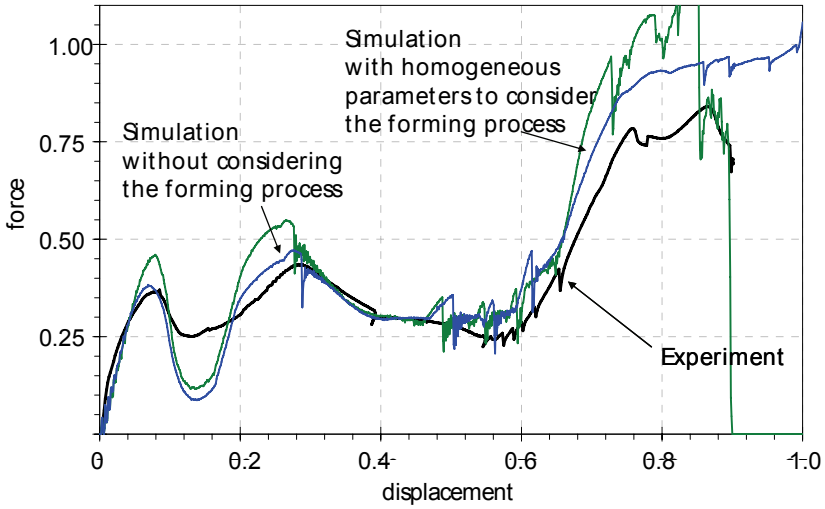

Figure 16: Tension-bearing test on a ZStE340 metal blank of a B-pillar: comparison of experiment (black curve), crash simulation without considering the forming process (blue), and crash simulation with considering the mapping scenario "global values" (green).

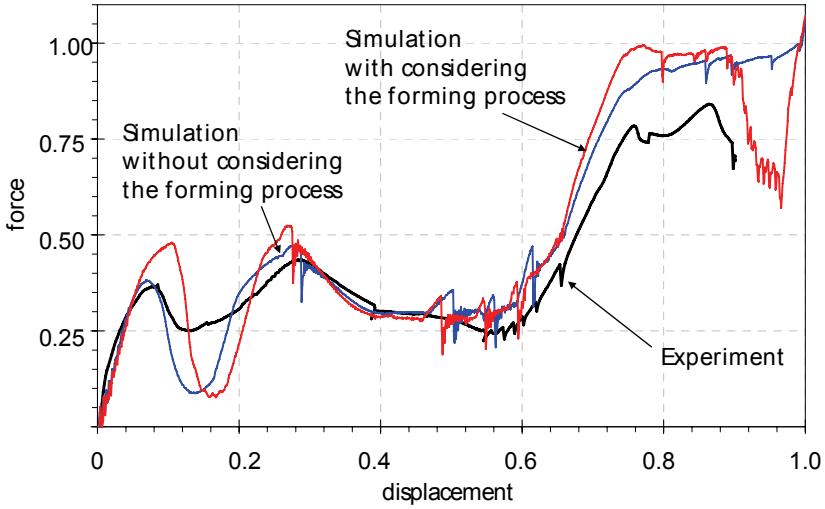

Figure 17: Tension-bearing test on a ZStE340 metal blank of a B-pillar: Comparison of experiment (black curve), crash simulation without considering the forming process (blue), and crash simulation with considering the mapping scenario "local thicknesses, strains (and damages)" (red).

4.5 Analysis of the Crash Simulations

As soon as all crash simulations have been completed, several analysis steps will be performed:

- stability analysis of the "final" crash model: a detailed analysis of instabilities as well as their backtracking by means of DIFF-CRASH technologies (based on the current version and also a considerably extended methodical library),
- DesParO's novel sensitivity analysis tool will be used in order
  - to check the quality of the mapped data base against variations coming from parameter sensitivities (cf. Section 3.1.3).
  - to analyze the simulation results of the crash simulations, the inputs of which have been prepared by step 8 in Section 2.2.2 and the mapping process. Particularly, the impact of the parameter variations on the crash simulation results (on fine grids) is analyzed.
  - to "physically" compress the crash simulation results, analogously to step 6 in Section 2.2.2.
- robustness analysis, based on appropriately defined measures.

5 Outlook

Further steps for analyzing the process chain forming to crash for the ZStE340 blank are
- a completion of the detailed analysis of the crash step, see Section 4.5,
- further comparisons to the related physical experiments from a statistical point of view,
- employment of an extended material model as described in Section 4.1.3.,
- an analysis of the whole process chain based on an extended set of input parameters,
- the setup of the overall multi-objective optimization scenario including robustness aspects,
- solution of the robust optimization task by means of DesParO,
- an analysis of the B-pillar itself.

The overall methodology will (continue to) prove its efficiency to predict statistics of the process chain, to reduce parameters and simulation data, as well as to robustly optimize the criteria chosen.

6 Acknowledgments

Parts of this work have been funded by the Fraunhofer MAVO CAROD (cf. [2] and [3]). The authors wish to thank Lialia Nikitina, Igor Nikitin and Clemens-August Thole (SCAI) and Dong-Zhi Sun (IWM) for fruitful discussions.

7 Literature

[1] Steffes-lai, D., Thole, C.-A., Nikitin, I., Nikitina, L.: “Interactive optimization with DesParO”, in: ERCIM News **73**, Special Theme “Maths for Everyday Life”, Väänänen, J., Trottenberg, U., eds., pp. 29-30, 2008.

[2] Burblies, A., Clees, T.: “ Computer Aided Robust Design – auf dem Weg zur simulierten Realität”, wt-online **1/2**, pp. 44-45, 2008.

[3] www.carod.fraunhofer.de

[4] Clees, T.: “Computer-Aided Robust Design for Multi-Disciplinary Processes” , Procs. 10th MpCCI Userforum, Feb. 17-18, Fraunhofer Institute for Algorithms and Scientific Computing SCAI, Sankt Augustin, Germany, pp. 22-31, 2009. Available from www.scai.fraunhofer.de/mpcci.

[5] Oeckerath, A.: “Enhanced multi-physics pre- and postprocessing tools”, Procs. 10th MpCCI Userforum, Feb. 17-18, Fraunhofer Institute for Algorithms and Scientific Computing SCAI, Sankt Augustin, Germany, 2009. Available from www.scai.fraunhofer.de/mpcci.

[6] Thole, C.-A.: “Reasons for scatter in crash simulation results”, 4th European LS-DYNA Users’ Conference, Ulm, Germany, 2003.

[7] www.scai.fraunhofer.de/femzip

[8] Müllerschön, H., Lorenz, D., Roux, W., Liebscher, M., Pannier, S., Roll, K.: “Probabilistic analysis of uncertainties in the manufacturing process of metal forming”, 6th European LS-DYNA Users’ Conference, 2007.

[9] Johnson, G.R., Cook, W.H.: “Fracture characteristics of three metals subjected to various strains, strain rates, temperatures and pressures”, Engineering Fracture Mechanics **21** (1), pp. 31-48, 1985.

[10] Bao, Y., Wierzbicki, T.: “On fracture locus in the equivalent strain and stress triaxiality space”, Int. J. Mech. Sci. **46** (81), pp. 81-98, 2004.

[11] Krasovskyy, A.: “Verbesserte Vorhersage der Rückfederung bei der Blechumformung durch weiterentwickelte Werkstoffmodelle”, Dissertation, University Karlsruhe, Germany, 2005.

[12] Neukamm, F., Feucht, M., Haufe, A.: “Consistent damage modelling in the process chain of forming to crashworthiness simulations”, 7th LS-DYNA Anwenderforum, Sep. 30 - Oct. 1, Bamberg, 2008.